Transcriptional Analysis of *serk1* and *serk3* Coreceptor Mutants[1]

G. Wilma van Esse[2], Colette A. ten Hove, Francesco Guzzonato, H. Peter van Esse[3], Mark Boekschoten[4], Lars Ridder[5], Jacques Vervoort, and Sacco C. de Vries*

Laboratory of Biochemistry, Wageningen University, 6708 WE Wageningen, The Netherlands

ORCID IDs: 0000-0001-5012-2346 (G.W.v.E.); 0000-0002-6110-2209 (C.A.t.H.); 0000-0002-6953-0523 (F.G.); 0000-0002-3667-060X (H.P.v.E.); 0000-0001-9454-775X (S.C.d.V.).

Somatic embryogenesis receptor kinases (SERKs) are ligand-binding coreceptors that are able to combine with different ligand-perceiving receptors such as BRASSINOSTEROID INSENSITIVE1 (BRI1) and FLAGELLIN-SENSITIVE2. Phenotypical analysis of *serk* single mutants is not straightforward because multiple pathways can be affected, while redundancy is observed for a single phenotype. For example, *serk1serk3* double mutant roots are insensitive toward brassinosteroids but have a phenotype different from *bri1* mutant roots. To decipher these effects, 4-d-old Arabidopsis (*Arabidopsis thaliana*) roots were studied using microarray analysis. A total of 698 genes, involved in multiple biological processes, were found to be differentially regulated in *serk1-3serk3-2* double mutants. About half of these are related to brassinosteroid signaling. The remainder appear to be unlinked to brassinosteroids and related to primary and secondary metabolism. In addition, methionine-derived glucosinolate biosynthesis genes are up-regulated, which was verified by metabolite profiling. The results also show that the gene expression pattern in *serk3-2* mutant roots is similar to that of the *serk1-3serk3-2* double mutant roots. This confirms the existence of partial redundancy between SERK3 and SERK1 as well as the promoting or repressive activity of a single coreceptor in multiple simultaneously active pathways.

The five somatic embryogenesis receptor kinase (SERK) receptors in Arabidopsis (*Arabidopsis thaliana*) are Leu-rich repeat receptor-like kinases that are involved in diverse processes such as somatic embryogenesis (Hecht et al., 2001), seedling development (Albrecht et al., 2008), plant immunity (Chinchilla et al., 2009), and stomatal patterning (Meng et al., 2015). SERK proteins function as ligand-binding coreceptors by heterodimerizing with different ligand-perceiving receptors (Chinchilla et al., 2009). Current models indicate that SERKs contribute to ligand binding by forming an integral part of the ligand-binding pocket (Santiago et al., 2013; Sun et al., 2013). This is most likely also the case for an increasing number of main ligand-perceiving receptors found to employ members of the SERK family in different plant families (aan den Toorn et al., 2015; Wang et al., 2015; Fan et al., 2016). SERK1, SERK3 (BAK1), and SERK4 (BKKI1) function as co-receptors of BRASSINOSTEROID INSENSITIVE1 (BRI1), which is the main ligand-perceiving receptor for brassinosteroids (BRs) in Arabidopsis (Wang et al., 2001; Li et al., 2002; Karlova et al., 2006; He et al., 2007). BRs are a class of plant-specific steroid hormones involved in cell elongation, division and differentiation, photosynthesis, stress responses, and senescence (Clouse and Sasse, 1998). Mutants unable to synthesize or perceive BRs have a dwarfed stature, are impaired in photomorphogenesis, and have fertility defects (Chory et al., 1991; Clouse et al., 1996; Clouse and Sasse, 1998).The BRI1-mediated BR signaling completely depends on its interaction with SERKs (Gou et al., 2012). However, with the exception of SERK3, single *serk* mutants do not give a morphological phenotype. Severe BR-related phenotypes are observed only in double or triple mutants of different SERK combinations, indicating that they act redundantly in BR signaling (Albrecht et al., 2008; Gou et al., 2012). An added complexity is that

[1] This work was supported by the IP/OP systems biology program of Wageningen University, the German Cluster of Excellence on Plant Sciences (grant no. EXC1028 to G.W.v.E.), and the Netherlands Proteomics Centre (to C.A.t.H.).

[2] Present address: Department of Plant Breeding and Genetics and Department of Plant Developmental Biology, Max Planck Institute for Plant Breeding Research, Carl-von-Linné-Weg 10, 50829 Cologne, Germany; and Cluster of Excellence in Plant Sciences, Heinrich-Heine-Universität Düsseldorf, Universitätsstrasse 1, 40255 Duesseldorf, Germany.

[3] Present address: Sainsbury Laboratory, Norwich Research Park, Norwich NR4 7UH, UK.

[4] Present address: Nutrition, Metabolism, and Genomics Group, Wageningen University, Stippeneng 4, 6708 WE Wageningen, The Netherlands.

[5] Present address: Netherlands eScience Center, Science Park 140 (Matrix I), 1098 XG Amsterdam, The Netherlands.

* Address correspondence to sacco.devries@wur.nl.

The author responsible for distribution of materials integral to the findings presented in this article in accordance with the policy described in the Instructions for Authors (www.plantphysiol.org) is: Sacco C. de Vries (sacco.devries@wur.nl).

G.W.v.E., H.P.v.E., and M.B. analyzed microarray data; C.A.t.H. performed qRT-PCR and physiological experiments; G.W.v.E. performed root length measurements; F.G., J.V., and L.R. performed metabolite extraction, mass spectrometry, and data analysis; G.W.v.E., F.G., L.R., and S.C.d.V. wrote the article; G.W.v.E., C.A.t.H., S.C.d.V., and L.R. designed research; all authors read and approved the final article.

www.plantphysiol.org/cgi/doi/10.1104/pp.16.01478

several members of the SERK family also serve in other signaling pathways, such as plant immunity (Heese et al., 2007; Chinchilla et al., 2009; Roux et al., 2011), male fertility (Albrecht et al., 2005), BR-independent cell death (He et al., 2007), abscission (Lewis et al., 2010), and root development (Du et al., 2012). This complicates the phenotypical analysis of *serk* mutants, especially in double and triple mutant combinations. Most studies performed so far are based on genetic and proteomic approaches. For example, a suppressor screen of the *nevershed* mutant, which does not show floral organ abscission, demonstrated that SERK1 functions as a negative regulator of abscission (Lewis et al., 2010). SERK3 has been identified as a coreceptor of BRI1 in a genetic screen for suppressors of a weak *bri1* phenotype and in a yeast two-hybrid screen (Nam and Li, 2002). SERK2 also can interact with BRI1; however, exogenous application of BR only enhanced SERK2 phosphorylation activity but not the amount of SERK2 interacting with BRI1. This suggests that SERK2 may have a less pronounced role in BR signaling revealed only in unnatural situations such as the overexpression of SERK2 or the exogenous application of BRs (Gou et al., 2012).

The BR-related phenotype of *serk3* can be enhanced by *serk1* (Albrecht et al., 2008; Du et al., 2012; Gou et al., 2012), while *serk4* enhances the defense- and cell death-related phenotype of *serk3* (Chinchilla et al., 2007; Heese et al., 2007; Roux et al., 2011). Several genes involved in cell cycle and root meristem differentiation, endodermis development, and auxin transport were found to be down-regulated in *serk* mutants. Because the root phenotype in double and triple *serk* mutants was found to be different from that in strong *bri1* mutant alleles, it was concluded that so far unknown BR-independent pathways requiring the SERK proteins are affected (Du et al., 2012).

Profiling of the global transcriptional changes in *bri1* null mutants has revealed a complex regulatory network integrating BR and light signaling pathways and showing multiple targets in the control of (root) development and cell elongation (Luo et al., 2010; Sun et al., 2010). This is in line with the proposed functions attributed to the BR signaling pathways.

To determine which BR-related and BR-unrelated processes are disturbed in *serk* mutants, a transcriptional analysis was performed. To simplify the interpretation, only *serk1* and *serk3* single and *serk1serk3* double mutants were used, and the analysis was restricted to roots rather than entire seedlings. The results show that a significant number of BR-related genes are differentially regulated in *serk1-3serk3-2* double mutants. In addition, transcriptional reprogramming occurred in the double mutants that appears to be unrelated to BR signaling and affects metabolic processes such as glycolipid and fatty acid metabolism. In particular, genes involved in suberin biosynthesis are down-regulated, while Met-derived glucosinolate biosynthesis genes are up-regulated, in *serk1-3serk3-2* double mutants. Hierarchical cluster (HCL) analysis showed that, in *serk3-2*, a similar but less pronounced regulation occurred that was not detected in *serk1-3*. Apparently, SERK3 affects metabolic processes in a BR-dependent and BR-independent fashion, suggesting that this single receptor serves even more pathways in a partially redundant mode with other SERK proteins.

RESULTS

The Magnitude of Differential Gene Expression Reflects the *serk* Mutant Root Phenotype

The phenotypes of the *serk* mutants have been described previously; *serk1-3serk3-2* has a severe reduction in root growth, which is minor in *serk3-2* and absent in *serk1-3* (Fig. 1A), largely comparable to that of *bri1* alleles (Supplemental Fig. S1A), corroborating data presented previously (Du et al., 2012; Gou et al., 2012). To determine which genes are differentially regulated in the *serk1* and *serk3* mutant lines, RNA isolated from roots of Col-0, *serk1-3*, and *serk3-2* single and double mutant seedlings was hybridized to Affymetrix GeneChip arrays (Hennig et al., 2003). Only genes differentially regulated more than 2-fold with a false discovery rate (FDR) of 1% significance were considered. RNA was isolated from roots cut just below the hypocotyl at 4 DAG, because at this time point, roots of the *serk3-2* single mutant already showed a reduction in root length (Fig. 1B). Out of more than 26,000 genes analyzed, only four and 42 genes were found to change expression in *serk1-3* and *serk3-2* mutant roots, respectively (Supplemental Table S1). Principal component analysis (PCA) of genes expressed in mutants and the wild type showed similar variation between experiments for all genes (Supplemental Fig. S2). In *serk1-3serk3-2* roots, 698 genes are differentially regulated (Supplemental Table S2), of which 29 also are differentially regulated over 2-fold in the *serk3-2* single mutant (Fig. 1C; Supplemental Table S3). The expression of a representative selection of these was confirmed by quantitative reverse transcription (qRT)-PCR (Supplemental Fig. S1). The majority of the 42 genes differentially regulated in the *serk3-2* single mutant display the same expression profile as in the *serk1-3serk3-2* double mutant (Fig. 1D). A comparison of all differentially regulated genes was made by HCL analysis (Eisen et al., 1998). Interestingly, the expression profile of *serk3-2* is very similar to that of the *serk1-3serk3-2* double mutant and differs only in magnitude (Fig. 1E). In contrast, the *serk1-3* mutant does not display this profile, suggesting that, in root development and at the transcriptional level, loss of SERK1 only has a measurable effect in the absence of SERK3.

Genes That Are Differentially Regulated in *serk3-2* and *serk1-3serk3-2*

The expression of all SERK genes was followed in *serk3-2* and *serk1-3serk3-2* mutant roots. The *serk1-3* mutant carries a T-DNA insertion in the coding sequence of

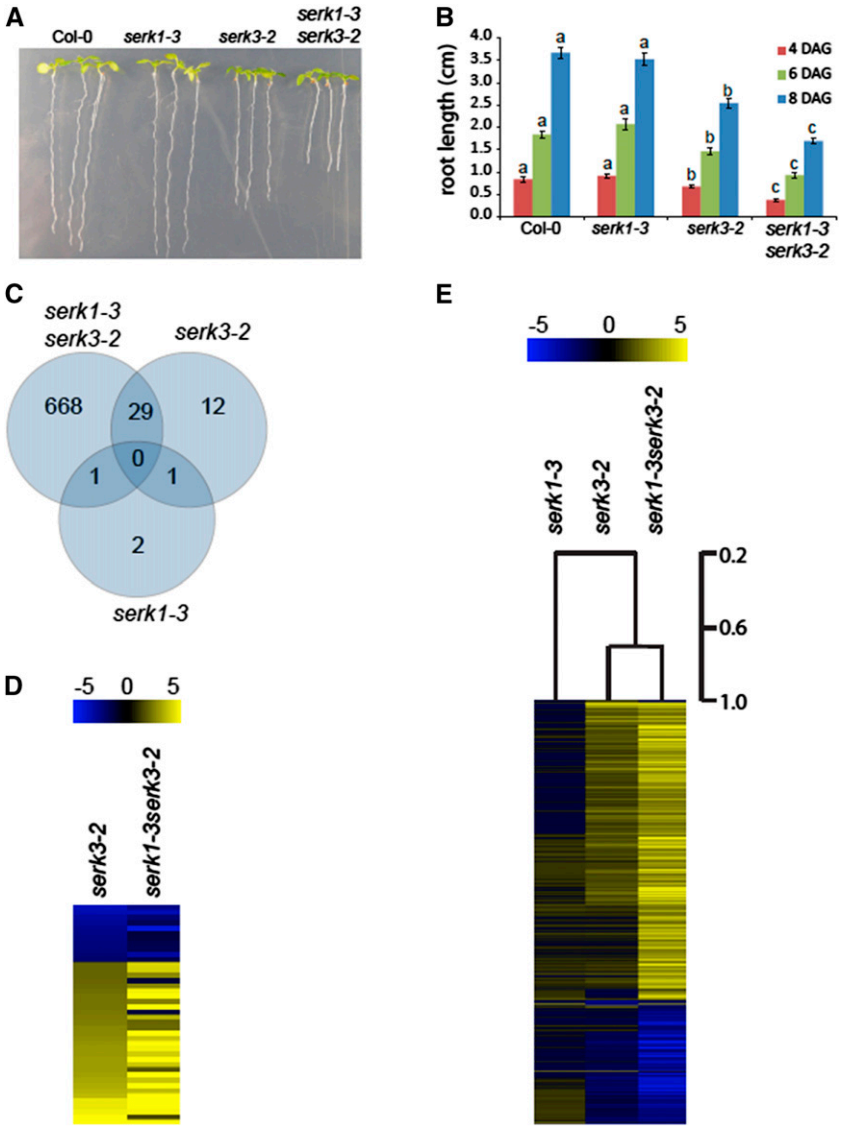

Figure 1. Morphological phenotype in *serk* mutants matches the magnitude of transcriptional response. A, Root lengths of *serk1-3*, *serk3-2*, and *serk1-3serk3-2* mutants compared with wild-type Columbia-0 (Col-0) at 8 d after germination (DAG). B, Statistical evaluation of the root lengths of *serk1-3*, *serk3-2*, and *serk1-3serk3-2* mutants at 4, 6, and 8 DAG. Lowercase a, b, and c indicate statistical differences. Data evaluation was done with a one-way ANOVA using a Bonferroni test ($\alpha = 0.05$). C, Venn diagram showing the overlap in significantly differentially regulated genes between the *serk1-3serk3-2* double mutant and the *serk1-3* and *serk3-2* single mutants. D, Heat map comparing genes differentially regulated in *serk3-2* with the *serk1-3serk3-2* double mutant. E, HCL analysis of all genes differentially regulated in the *serk1-3* and *serk3-2* single mutants and the *serk1-3serk3-2* double mutant. All HCL plots were made using $\log_2$ fold change values. For all root length measurements, error bars indicate SE; 20 or more roots were measured in three independent replicates.

the SERK1 gene and, therefore, does not block the formation of the transcript. Surprisingly, SERK1 (AT1G71830) transcripts are significantly higher in the *serk1-3serk3-2* mutant (2.4-fold change, FDR < 0.01), as are, to a lesser extent, SERK4 (AT2G13790) transcripts (1.6-fold change, FDR = 0.05). This possibly represents a compensatory mechanism for the loss of active SERK1 and SERK3 protein.

Genes differentially regulated in the *serk3-2* mutant are involved in various cellular processes, such as photosynthesis, transport, and protein degradation (Supplemental Table S4). To assess if these genes are part of a certain biochemical pathway, an overrepresentation analysis (ORA) was performed (Backes et al., 2007; van Esse et al., 2009; Hanssen et al., 2011). In the *serk3-2* mutant, overrepresentation of photosynthesis and metabolic pathways was noted among the up-regulated genes, whereas none was found in the down-regulated gene categories. In the double mutant, additional categories were found to be overrepresented, mainly those involved in energy metabolism and in glucosinolate biosynthesis. In addition, down-regulated genes were found to be involved in secondary metabolite biosynthesis (Table I).

The overrepresentation of photosynthesis genes suggests a link between SERK activity, BR signaling, and chloroplast development. Light-grown roots have the capacity to develop chloroplasts (Kobayashi et al., 2012). BR signaling is correlated with the response to light; in the BR biosynthesis mutant *deetiolated2*, for example, increased expression of light-responsive genes was observed (Chory et al., 1991; Song et al., 2009). Furthermore, BR up-regulated transcriptional activation of BZR1 and BES1/BZR2 represses the expression of positive regulators of light signaling and induces the expression of negative ones (Luo et al., 2010; Sun et al., 2010; Wang et al., 2012). Hence, reduced BR signaling apparently results in an increase in the expression of genes involved in photosynthesis.

Table I. *ORA of differentially regulated genes in serk1-3serk3-2 and serk3-2*

Category	Expected	Observed	*P*
serk3-2 up-regulated			
Photosynthesis	0	5	3.6×10^{-08}
Metabolic pathways	3	6	4.1×10^{-02}
serk1-3serk3-2 up-regulated			
Photosynthesis	2	26	2.1×10^{-25}
Photosynthesis antenna proteins	1	14	1.5×10^{-15}
Carbon fixation in photosynthetic organisms	3	16	9.3×10^{-08}
Metabolic pathways	51	79	9.3×10^{-08}
Porphyrin and chlorophyll metabolism	2	8	5.5×10^{-04}
Glyoxylate and dicarboxylate metabolism	1	6	2.1×10^{-03}
Glucosinolate biosynthesis	1	4	1.5×10^{-02}
serk1-3serk3-2 down-regulated			
Glycerolipid metabolism	0	5	6.4×10^{-05}
Glycerophospholipid metabolism	0	5	3.2×10^{-04}
Phe metabolism	1	6	4.9×10^{-04}
Biosynthesis of secondary metabolites	7	15	7.4×10^{-04}
Phenylpropanoid biosynthesis	1	6	7.4×10^{-04}
Fatty acid metabolism	0	3	5.0×10^{-03}
Metabolic pathways	12	18	1.0×10^{-02}
Limonene and pinene degradation	1	3	2.6×10^{-02}
Stilbenoid, diarylheptanoid, and gingerol biosynthesis	1	3	2.6×10^{-02}

Next, the genes differentially regulated in *serk3-2* and *serk1-3serk3-2* were compared with published data sets on (putative) targets of BZR1/BES1 and differentially regulated genes in the BRI1 null mutant *bri1-116* (Sun et al., 2010; Yu et al., 2011; Fig. 2; Supplemental Fig. S3; Supplemental Table S5; Supplemental File S1). In total, 331 differentially regulated genes were observed in the *serk1-3serk3-2* mutant that are BR related (Tables II and III). This is a significantly higher number than would be expected by chance alone (124 genes; Table III) and indicates that the BR signaling process is significantly affected in roots of the *serk1-3serk3-2* mutants. The majority of up-regulated photosynthesis-related genes identified in the ORA are BR related, while a number of BR-related metabolic processes appear to be significantly down-regulated (Table II). Interestingly, genes reported to participate in BR-related as well as non-BR-related up-regulated metabolic pathways appear to be up-regulated in *serk* mutant roots. This category includes genes involved in the biosynthesis of glucosinolates, secondary metabolites, fatty acid metabolism, and glyoxylate and dicarboxylate metabolism (Table II).

Genes Differentially Regulated in the Weak Allelic *bri1-301* Mutant

Macroscopically, *bri1-301* has a phenotype comparable to that of wild-type seedlings while showing insensitivity toward exogenously applied BRs (Xu et al., 2008; van Esse et al., 2012). To assess whether roots of the *bri1-301* mutant have a transcriptional phenotype at physiological ligand concentrations, an analysis of this mutant was included (Supplemental Tables S1 and S2). Genes differentially regulated in the *bri1-301* mutant compared with the wild type were compared with those affected in the *bri1-116* mutant and the *serk1* and *serk3* single and double mutants. In *bri1-301* roots, only four genes were seen to be differentially regulated (Supplemental Table S6). This is significantly less compared with the data set available for the strong *bri1-116* mutant, where 3,531 genes (1.5-fold cutoff and FDR $<$ 0.01) are affected (Sun et al., 2010). The *bri1-116* data set obtained from the literature was constructed using a lower cutoff and FDR value than used in our analyses. The rationale behind this was that BR-regulated genes do not show extensive transcriptional responses (Deng et al., 2007). However, using a cutoff value of 1.5-fold change (FDR $<$ 0.01) did not increase the number of differentially regulated genes found in *bri1-301* in two independent experiments (Supplemental Table S6). HCL analysis using *bri1-301*, *serk3-2*, and *serk1-3serk3-2* did not show a clear correlation, due to the absence of a clear transcriptional profile in the *bri1-301* mutant (Fig. 2B). In conclusion, although *bri1-301* roots are BR insensitive, hardly any effect on transcriptional response is observed.

Global Transcriptional Analyses of Other SERK1- and SERK3-Affected Processes

SERK1 and SERK3 are important components in processes other than BR1-mediated signaling, such as abscission, cell death, and defense. Since these processes have been well studied, readily available data sets of global transcriptional changes are available in the Gene Expression Omnibus (GEO), The Arabidopsis Information Resource (TAIR), and the literature (Edgar et al., 2002; Zipfel et al., 2004; Denoux et al., 2008; Boudsocq et al., 2010; Lamesch et al., 2012; Niederhuth et al., 2013). Transcriptional changes due to the absence of functional HAESA (HAE) and HAESA-LIKE (HSL2)

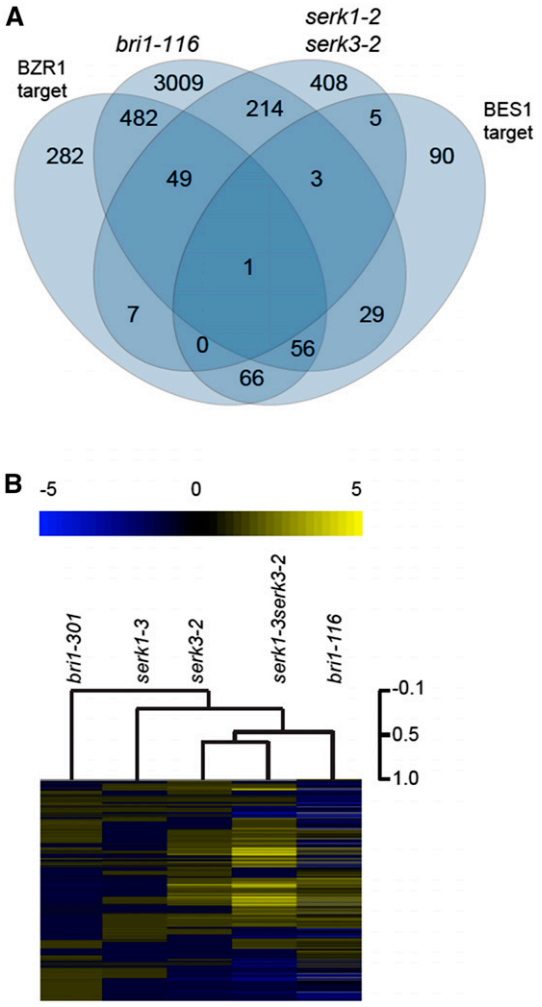

Figure 2. Comparison of differentially regulated genes in the *serk1-3serk3-2* mutant with BR-related genes. A, Venn diagram showing genes differentially regulated in the *bri1-116* mutant and known BR-related BES1 and BZR1 target genes compared with the *serk1-3serk3-2* double mutant. B, HCL analysis comparing genes differentially regulated in the *bri1-116* and *bri1-301* mutants with the *serk3-2* and *serk1-3serk3-2* mutants. Yellow indicates up-regulated and blue indicates down-regulated. Data on BR-related BES1/BZR1 target genes and genes differentially regulated in the *bri1-116* mutant were derived from Yu et al. (2011) and Sun et al. (2010).

receptor-like kinases and known abscission-related genes derived from TAIR were used as a reference set for abscission-related genes (Patterson, 2001; Sun and van Nocker, 2010; González-Carranza et al., 2012; Niederhuth et al., 2013; Kumpf et al., 2013). *haehsl2* double mutants fail to abscise their floral organs (Jinn et al., 2000; Cho et al., 2008; Stenvik et al., 2008). The defense-related gene set consists mainly of genes that are differentially regulated upon flg22 treatment (Zipfel et al., 2004; Denoux et al., 2008; Boudsocq et al., 2010). Known cell death-related genes were derived from TAIR (Lamesch et al., 2012). This list was extended using differentially regulated genes in a *constitutive expresser of PR genes5* (*cpr5*) mutant downloaded from the GEO database (Edgar et al., 2002). *cpr5* mutants have several phenotypes, including spontaneous cell death and defects in cell division, cell expansion, and cell wall biogenesis (Bowling et al., 1997; Kirik et al., 2001; Gao et al., 2011). Although none of these processes are described to occur in roots, the corresponding genes may nonetheless be differentially regulated. As mentioned previously, *serk1-3serk3-2* has a reduced root length and fewer meristematic cells (Du et al., 2012; Gou et al., 2012). One possible cause for the meristem phenotype of *serk1-3serk3-2* is reduced cell cycle progression in the root meristem cells, as postulated previously for the *bri1-116* mutant (González-García et al., 2011). In addition, it has been proposed that SERKs affect cell cycle and division via BR-independent processes (Du et al., 2012). Therefore, we also included previously described core cell cycle/cell differentiation genes as well as known cell cycle- and cell differentiation-related genes in TAIR in our analysis (Vandepoele et al., 2002).

The reference sets thus obtained (Supplemental Tables S8–S11) were compared with the transcriptional changes monitored in root tissue of the *serk1-3serk3-2* double mutant (for *P* values, see Table III). Subsequently, it was determined whether an overlap in the resulting set of differentially regulated genes exists with BR- and non-BR-related processes (Fig. 3). From the 209 core cell cycle genes in the reference sets, only five genes were differentially regulated in the absence of SERK1 and SERK3 (Fig. 3), suggesting that cell cycle activity is not a major target of the SERK1 and SERK3 genes (Table III). However, when the expression of a number of genes was tested by qRT-PCR, both CYCLIN D1;1 (CYCD1;1) and CYCB1;1 were found to be down-regulated in *serk1-3serk3-2* mutant roots (Supplemental Fig. S1B). *cycd1;1* mutants show a defect in seed germination and a significant delay in the onset of cell proliferation (Masubelele et al., 2005), phenotypes that have not been observed in *serk1-3serk3-2* mutants. If cell division activity is affected in the absence of SERK1 and SERK3, this may be a rather subtle effect. Similarly, only a small overlap was observed between genes involved in abscission, cell death, and defense and the differentially regulated genes in the *serk1-3serk3-2* double mutant (Fig. 3). For abscission- and cell death-related genes, no significant categories were identified in the ORA using GeneTrail. Comparison between the differentially regulated genes in *serk1-3serk3-2* root tissue with flagellin-responsive genes suggested that there was a significant up-regulation of this biological process (Table III). However, when performing an ORA using GeneTrail software on the 44 genes overlapping between these data sets, it appears that they are involved mainly in secondary metabolism rather than a core defense process. Noteworthy, a number of acetyltransferases were identified in the comparison between the abscission-related data set and the differentially regulated genes in *serk1-3serk3-2* roots. For example, GLYCEROL-3-PHOSPHATE-3-PHOSPHATE

Table II. *ORA of BR-related and non-BR-related genes differentially regulated in serk1-3serk3-2 double mutants*

Category	Expected	Observed	*P*
serk1-3serk3-2 BR-related up-regulated			
Photosynthesis	1	21	5.50E-20
Photosynthesis, antenna proteins	1	11	1.60E-12
Metabolic pathways including glucosinolates	3	34	2.90E-04
Porphyrin and chlorophyll	1	7	2.90E-04
Carbon fixation in photosynthetic organisms	2	6	4.00E-02
serk1-3serk3-2 BR-related down-regulated			
Biosynthesis of secondary metabolites	3	8	7.00E-03
Phe metabolism	1	3	1.00E-02
Phenylpropanoid biosynthesis	1	3	1.00E-02
serk1-3serk3-2 non-BR-related up-regulated			
Glyoxylate and dicarboxylate metabolism	0	4	5.00E-05
Carbon fixation in photosynthetic organisms	0	4	1.00E-03
Biosynthesis of secondary metabolites	4	9	8.00E-03
Metabolic pathways	6	11	3.00E-02
serk1-3serk3-2 non-BR-related down-regulated			
Fatty acid metabolism	0	3	1.00E-03
Metabolic pathways	5	11	2.00E-03

SN-2-ACYLTRANSFERASE5 (GPAT5) and FATTY ACID REDUCTASE4 (FAR4) and FAR5 are acetyltransferases essential for the biosynthesis of suberin (Beisson et al., 2007; Domergue et al., 2010). Genes besides GPAT5 (AT3G11430; Li et al., 2007; Beisson et al., 2012) known to be involved in suberin and cutin biosynthesis also were checked (Supplemental Table S7). Suberin in roots and cutin in leaves are secondary wall modifications that help make plant organs waterproof. A comprehensive review of the current knowledge of both processes is available (Beisson et al., 2012; Vishwanath et al., 2015). Of the 11 genes known to be involved in suberin biosynthesis, all but two are differentially regulated 2-fold (FDR < 0.01; Supplemental Fig. S4A). Suberin mutants such as *gpat5* have a more permeable seed coat (Beisson et al., 2007). However, tetrazolium salt staining failed to demonstrate a similar phenotype in *serk1-3serk3-2* mutants (Supplemental Fig. S4C).

Aliphatic Glucosinolates Increase in *serk1-3serk3-2* Double Mutants

The ORA of genes differentially regulated in *serk1-3serk3-2* indicates that the glucosinolate biosynthesis is partly stimulated in this mutant. In particular, four of the genes up-regulated in *serk1-3serk3-2* encode enzymes involved in the biosynthesis of Met-derived aliphatic glucosinolates (Fig. 4). The branched chain amino acid aminotransferase (BCAT4) constitutes the first reaction of this pathway, catalyzing the deamination of Met to the corresponding 2-oxo acid in the cytoplasm. The second up-regulated gene, MAM1, is involved in the first three chain elongation steps of the 2-oxo acid in the chloroplast. The up-regulated CYP79F2 and CYP83A1 genes constitute the first steps of the core pathway to form the aliphatic glucosinolates from the chain-elongated amino acid, being aldoximated by the cytochromes P450 of the CYP79 family (Knoke et al., 2009). While CYP79F1

Table III. *ORA on (known) SERK1- and SERK3-related processes*

Presented are the number of genes in the reference set (Refset), the number of genes to be found by chance based on the size of the reference set, the number of differentially regulated genes (698 in *serk1-3serk3-2*) and the 27,827 genes represented on the GeneChip (Expected), the number of genes actually found (Observed), and the corresponding *P* values calculated using a cumulative hypergeometric distribution.

Category	Refset	Expected	Observed	*P*
BR signaling	4,947	124	331	6.5×10^{-75}
BR signaling *bri1-116*	3,550	89	267	4.7×10^{-67}
BR signaling BZR1 target	955	24	69	3.7×10^{-15}
BR signaling BES1 target	250	6	9	1.0×10^{-01}
Abscission	410	10	23	3.2×10^{-04}
Cell cycle	209	5	5	6.0×10^{-01}
Cell death	439	11	14	2.2×10^{-01}
Defense	1,354	34	44	4.9×10^{-02}
Suberin and cutin biosynthesis	30	1	16	2.2×10^{-18}
Suberin biosynthesis	11	0	9	2.0×10^{-13}

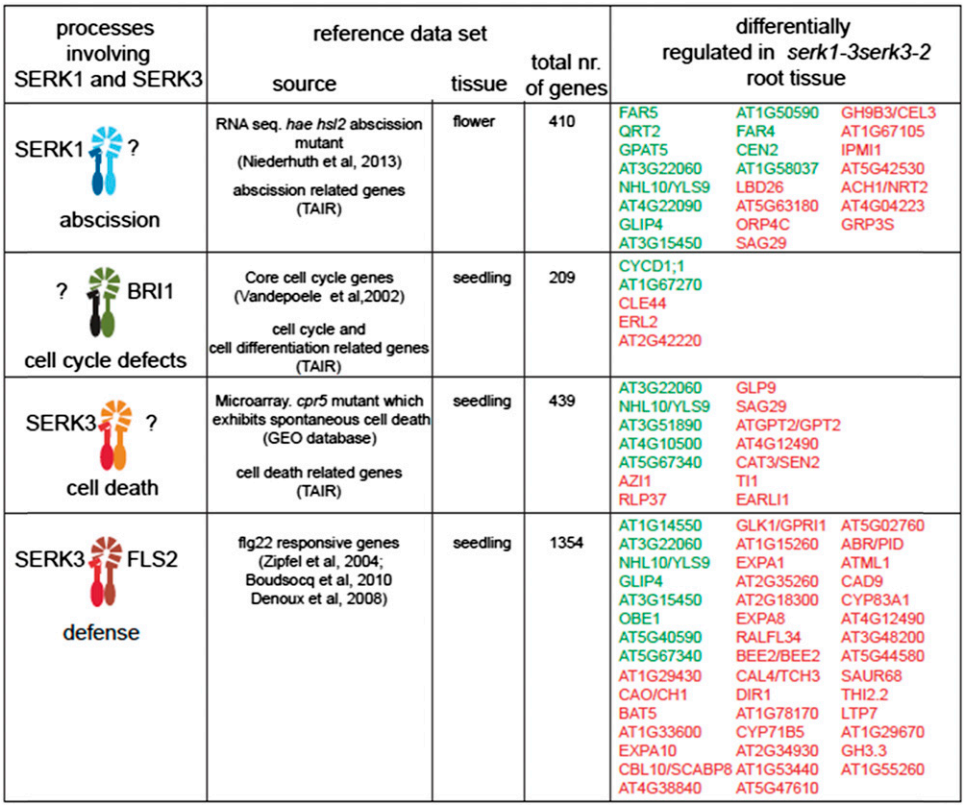

processes involving SERK1 and SERK3	reference data set: source	tissue	total nr. of genes	differentially regulated in *serk1-3serk3-2* root tissue
SERK1 ? abscission	RNA seq. *hae hsl2* abscission mutant (Niederhuth et al, 2013); abscission related genes (TAIR)	flower	410	FAR5, QRT2, GPAT5, AT3G22060, NHL10/YLS9, AT4G22090, GLIP4, AT3G15450, AT1G50590, FAR4, CEN2, AT1G58037, LBD26, AT5G63180, ORP4C, SAG29, GH9B3/CEL3, AT1G67105, IPMI1, AT5G42530, ACH1/NRT2, AT4G04223, GRP3S
? BRI1 cell cycle defects	Core cell cycle genes (Vandepoele et al,2002); cell cycle and cell differentiation related genes (TAIR)	seedling	209	CYCD1;1, AT1G67270, CLE44, ERL2, AT2G42220
SERK3 ? cell death	Microarray. *cpr5* mutant which exhibits spontaneous cell death (GEO database); cell death related genes (TAIR)	seedling	439	AT3G22060, NHL10/YLS9, AT3G51890, AT4G10500, AT5G67340, AZI1, RLP37, GLP9, SAG29, ATGPT2/GPT2, AT4G12490, CAT3/SEN2, TI1, EARLI1
SERK3 FLS2 defense	flg22 responsive genes (Zipfel et al, 2004; Boudsocq et al, 2010 Denoux et al, 2008)	seedling	1354	AT1G14550, AT3G22060, NHL10/YLS9, GLIP4, AT3G15450, OBE1, AT5G40590, AT5G67340, AT1G29430, CAO/CH1, BAT5, AT1G33600, EXPA10, CBL10/SCABP8, AT4G38840, GLK1/GPRI1, AT1G15260, EXPA1, AT2G35260, AT2G18300, EXPA8, RALFL34, BEE2/BEE2, CAL4/TCH3, DIR1, AT1G78170, CYP71B5, AT2G34930, AT1G53440, AT5G47610, AT5G02760, ABR/PID, ATML1, CAD9, CYP83A1, AT4G12490, AT3G48200, AT5G44580, SAUR68, THI2.2, LTP7, AT1G29670, GH3.3, AT1G55260

Figure 3. Global transcriptional analysis of non-BR-related processes involving SERK1 and SERK3. Comparison is shown for the global transcriptional responses during abscission, cell cycle and differentiation, cell death, and defense with differentially regulated genes in the *serk1-3serk3-2* double mutant. Data on genes involved in abscission, cell cycle, cell death, and defense were derived from the literature or reference data sets available in the GEO and TAIR. Red type indicates up-regulated and green type indicates down-regulated.

shows no chain length specificity, the *serk1serk3* up-regulated CYP79F2 selectively catalyzes this reaction for long-chain glucosinolates. Next, oxidation by the *serk1serk3* up-regulated CYP83A1 converts the aldoximes to active compounds. A subsequent conjugation with a sulfur donor can occur nonenzymatically using glutathione as a substrate. The produced *S*-alkylthiohydroxymates are converted to thiohydroxymates, glucosylated, and sulfated to give rise to glucosinolates, which then can be further modified by *S*-oxidation, resulting in sulfoxide glucosinolates (Halkier and Gershenzon, 2006; Sønderby et al., 2010). Induction of BCAT4, MAM1, CYP79F2, and CYP83A1 gene expression could result in an increase in aliphatic glucosinolate biosynthesis in the *serk1-3serk3-2* mutant. To verify this hypothesis, glucosinolate levels were determined by comparative liquid chromatography-mass spectrometry profiling in methanol extracts of Col-0 and *serk1-3serk3-2* root tissue. Based on both univariate and multivariate analyses of the data sets, a total of 12 Met-derived aliphatic glucosinolates are increased significantly in *serk1-3serk3-2*. These include most of the short-chain glucosinolates, either in the thioether or the sulfoxide form, as well as the long-chain 8-methylsulfinyloctyl glucosinolate, all of which are downstream products of the up-regulated genes (Fig. 4A). In addition, a parallel increase of the 2-oxo-5-methylpentanoate intermediate and a decrease of the sulfate donor glutathione are detected. The same response was not observed for all four identified Trp-derived glucosinolates (Table IV). Enrichment analysis performed on all the identified metabolites confirms the glucosinolate biosynthesis pathways as significantly regulated, with a P value of 4.715×10^{-7}.

DISCUSSION

In this study, we employed a transcriptional analysis using microarrays to identify biological processes involving SERK1 and SERK3. This approach resulted in the identification of known BR-related genes, indicating the robustness of the analysis. In addition, *serk1serk3* mutants were found to be affected in a secondary metabolic process such as glucosinolate biosynthesis. One major challenge in studying the gene regulation of receptor mutants is that the effects may be caused indirectly by the differential regulation of transcription factors downstream of the receptor. This is complicated even further by the interaction of SERK coreceptors with different main ligand-perceiving receptors, thereby affecting multiple signaling pathways. This raises the question of whether all signal transduction pathways mediated by SERK coreceptors can truly be separated using genetic approaches. To simplify the analysis in our studies, only entire roots were used from light-grown seedlings, in contrast to the transcriptional analyses done on *bri1-116* whole seedlings that were compared after growth in complete darkness (Sun et al., 2010). Together with the fact that phenotypical effects in *bri1*

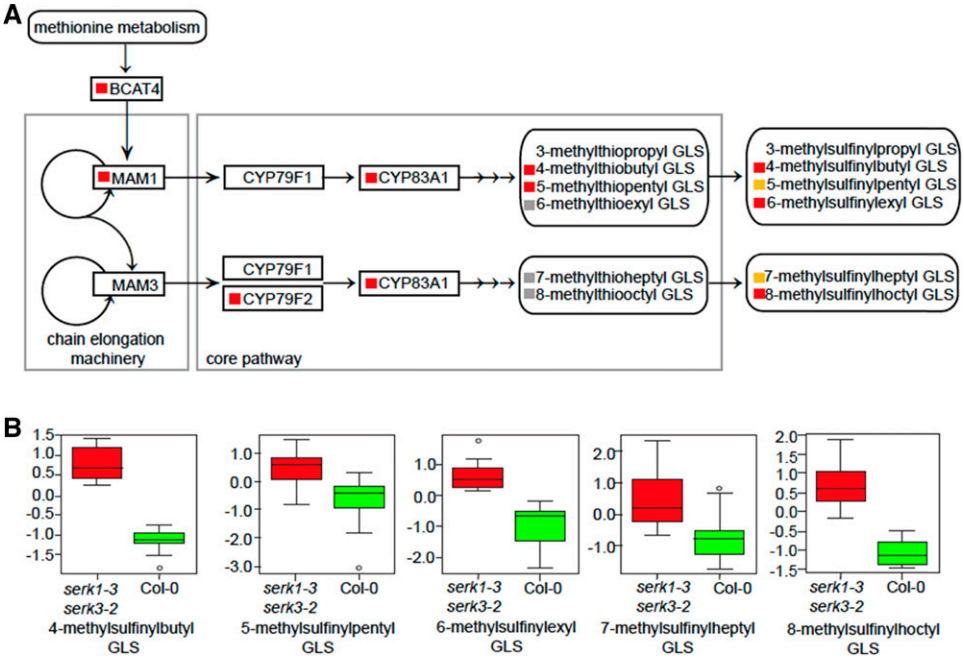

Figure 4. Aliphatic glucosinolate levels are higher in the *serk1-3serk3-2* mutant. A, Biosynthesis pathway of Met-derived aliphatic glucosinolates adapted from the KEGG database. Highlighted with red squares are significantly up-regulated genes and corresponding increased amounts of glucosinolates; highlighted with yellow squares are glucosinolates that were only significant in univariate analysis without Bonferroni correction; and highlighted with gray squares are those that were detected but for which peak intensity did not differ significantly. B, Box plots of autoscaled intensities of the five sulfinyl glucosinolates (GLS) detected in the *serk1-3serk3-2* mutant (red) and in the Col-0 control (green).

mutant roots appear to be more pronounced in only a small number of cells in the meristem, this most likely explains why, in our analysis, the number of genes found to be differentially expressed in the weak mutant *bri1-301* and in the *serk1* and *serk3* mutants is modest and only a subset of the entire transcriptome affected by BRs.

Phenotypically, only *serk3* single mutant lines show a reduced root growth phenotype, whereas roots of *serk1* single mutants do not have a phenotype. On the other hand, *serk1serk3* double mutants have a severe root growth phenotype (Du et al., 2012; Gou et al., 2012). Monitoring the transcriptional response using microarray analysis shows that *serk3-2* single mutants display distinct transcriptional changes while the *serk1-3* single mutants do not. Only when SERK1 and SERK3 are both disrupted is a significant increase in differentially regulated genes observed. Remarkably, the transcriptional

Table IV. *Univariate and multivariate analysis of glucosinolate-related metabolites in serk1serk3 4-DAG root tissue extracts*

RF, Random forest; SAM, significant analysis of microarrays. The *P* value for significance in univariate analysis with Bonferroni correction is 2.2×10^{-4}.

Rank	Glucosinolate	Fold Change	*P*	SAM Rank	RF Rank
Significant in multivariate analysis and/or univariate analysis with Bonferroni correction					
1	4-Methoxy-3-indolylmethyl glucosinolate	1.8	3.26×10^{-11}	1	8
5	8-Methylsulfinyloctyl glucosinolate	1.7	1.38×10^{-7}	12	6
7	4-Methylsulfinylbutyl glucosinolate	1.8	3.86×10^{-10}	2	25
24	6-Methylsulfinylhexyl glucosinolate	1.5	6.79×10^{-4}	27	27
45	Glutathione	0.6	2.60×10^{-4}	37	48
46	4-Methylthiobutyl glucosinolate	2.0	6.41×10^{-6}	53	23
50	5-Methylthiopentyl glucosinolate	1.7	3.58×10^{-4}	47	63
54	3-Butenyl glucosinolate	1.6	–	39	–
62	2-Oxo-5-methylpentanoate	1.4	–	42	61
>70	4-Benzoyloxybutyl glucosinolate	0.7	–	66	–
>70	1-Methoxy-3-indolylmethyl glucosinolate	0.8	–	69	–
Significant in multivariate analysis without Bonferroni correction					
	5-Methylsulfinylpentyl glucosinolate	1.6	2.01×10^{-3}	–	–
	7-Methylsulfinylheptyl glucosinolate	2.5	8.18×10^{-3}	–	–
No significant difference					
	6-Methylthioexyl glucosinolate				
	7-Methylthioheptyl glucosinolate				
	8-Methylthiooctyl glucosinolate				
	4-Hydroxy-3-indolylmethyl glucosinolate				
	Indolylmethyl glucosinolate				

profile of the *serk1-3serk3-2* double mutant emulates the profile of the *serk3-2* mutant but displays transcriptional changes of a higher magnitude. Together, this demonstrates that the global transcriptional profiles resemble the macroscopically observed phenotypes. Both at the phenotypic and transcriptional levels, loss of SERK1 only affects root growth in the absence of SERK3. The presence of SERK1 does provide a certain robustness to the system, since it can partially rescue a SERK3 mutant phenotype and ameliorate the transcriptional changes in this mutant. Similarly, in other tissues, other combinations of SERKs may display similar profiles. Indeed, the rosette phenotype of the *serk1serk3* double mutant is more severe compared with that of the *serk3* single mutant (Gou et al., 2012), and the defense phenotype of *serk3* is enhanced by *serk4* while the *serk4* single mutant does not have a phenotype (Chinchilla et al., 2007; Heese et al., 2007; Roux et al., 2011).

Preventing the production of functional SERK proteins resulted in increased transcription or reduced degradation of the corresponding truncated mRNAs or, in one case, increased transcription of another member of the family. A similar phenomenon was noted previously in the analysis of the SERK family (Jeong et al., 2010) and may suggest a form of feedback control.

A significant number of genes that are differentially regulated in the absence of SERK1 and SERK3 are BR related. From the root growth and BL insensitivity phenotype, it is evident that roots of the *serk1-3serk3-2* double mutant exhibit a BR-related phenotype. In total, about 58% of the genes differentially regulated in the absence of SERK3 also are differentially regulated in a *bri1-116* mutant or known as targets of BES1/BZR1. In addition, a number of photosynthesis-related genes are significantly up-regulated in root tissue of *serk3-2* and *serk1-3serk3-2* mutants and in a *bri1-116* null mutant. This suggests that photosynthesis-related genes that are differentially regulated in the absence of SERK1 and SERK3 are the results of impaired BR signaling. This is in line with the negative regulation of light-responsive genes by BRI1-mediated BR signaling via the activation of BES1/BZR1 (Luo et al., 2010; Sun et al., 2010; Wang et al., 2012). An impaired BR signaling due a reduction in either receptor or ligand levels results in an increased expression of light-responsive genes (Chory et al., 1991; Song et al., 2009).

BRI1 also is known to be involved in cell cycle progression and cell differentiation in the root meristem (González-García et al., 2011; Hacham et al., 2011). In the *serk1-3serk3-2* double mutants, the cell cycle- and cell differentiation-related genes CYCD1;1 and AT1G67270 are differentially up-regulated and CLAVATA3/ESR-RELATED44, ERECTA-LIKE2, and AT2G42220 are differentially down-regulated. CYCD1;1, which in the wild-type situation is up-regulated at the start of cell division, is involved in the onset of cell proliferation during seed germination, resulting in a delayed germination in the *cycd1;1* mutants (Masubelele et al., 2005). In the *serk1-3serk3-2* mutant, CYCD1;1 is down-regulated, suggesting that the onset of cell division may be impaired. However, the ORA demonstrates that cell cycling and differentiation are not disrupted significantly in the *serk1-3serk3-2* double mutant. This suggests that, if the cell cycle and differentiation are disrupted in the *serk1-3serk3-2* double mutant, it is most likely through a subtle effect on a small number of core cell cycle genes. Here, CYCB1;1 expression remains unaffected in the microarray experiments and shows significant down-regulation by qRT-PCR, while previously, it was reported that *serk1serk3* roots show increased expression of CYCB1;1 (Du et al., 2012). What causes this apparent discrepancy is unclear; it may be due to differences in material sampling procedures. Noteworthy, differences in the identification of cell cycle markers in *bri1* mutants have been reported previously. For example, the *bri1* null mutant *bri1-701* does not show altered CYCB1;1 levels according to the qRT-PCR data of Du et al. (2012), while the expression of the same marker is reduced by about 50% in the *bri1-116* mutant using a reporter line (Hacham et al., 2011).

In the ORA performed on non-BR-related genes, it appears that metabolic pathways involving the biosynthesis of secondary metabolites and glyoxylate and dicarboxylate metabolism are affected. These genes are neither listed as direct targets of BZR1/BES1 nor affected in the *bri1-116* mutant (Sun et al., 2010); therefore, they are classified as non-BR-related genes in this study. A number of genes found here appear to be related to BR-related cell wall modifications (Wolf et al., 2012); others, such as GPAT5, FAR4, and FAR5, are abscission related. These genes are essential for suberin biosynthesis, a process required to protect the abscission zone with a layer of suberin and lignin (Roberts et al., 2000). In line with our observations are the role of SERK1 as a negative regulator of abscission in Arabidopsis flowers (Lewis et al., 2010) and the finding that *serk1serk3serk4* triple mutants display defects in floral organ abscission (Meng et al., 2016). Suberin functions as a protective barrier not only in abscission zones but also in root tissues (Beisson et al., 2012). Suberin, a cutin-like fatty acid- and glycerol-based polymer, forms part of the protective barrier against pathogens, and the transport of water and solutes forms the extracellular environment (Höfer et al., 2008; Baxter et al., 2009). While all known suberin and cutin biosynthesis genes (Beisson et al., 2012) were significantly down-regulated in roots of the *serk1-3serk3-2* double mutant, seed coat permeability remains unaltered compared with the wild type. This suggest that there is a form of physiological redundancy in suberin biosynthesis perhaps dependent on its developmental context.

In roots of the *serk1-3serk3-2* double mutant, the glucosinolate biosynthesis genes CYP79F2, MAM1, BCAT4, and CYP83A1 are significantly up-regulated. In agreement with these findings, significantly higher levels of several Met-derived aliphatic glucosinolates are observed in the *serk1-3serk3-2* double mutants. This is in line with the observations made with BRI1 receptor mutants (Guo et al., 2013), suggesting that the SERK1

and SERK3 coreceptors are clearly involved in this aspect of BR signaling. Direct comparison of metabolomics with other omics data often is not straightforward (Fernie and Stitt, 2012). Some prerequisites for the successful correlation of transcriptomics and metabolomics results appear to be met in our study. First, the detected glucosinolates are the end points of a regulated pathway; consequently, their levels are expected to reflect differences in the metabolic flux through this pathway. Second, at least one of the regulated enzymes should control the flux through the glucosinolate pathway. Olson-Manning et al. (2013) reported that CYP79F1, catalyzing the first step in the core pathway, mainly controls the flux toward short-chain aliphatic glucosinolates. The related gene encoding CYP79F2, which is up-regulated in our study, only controls the biosynthetic flux of longer chain glucosinolates (Chen et al., 2003; Olson-Manning et al., 2013). Since the levels of both short- and long-chain aliphatic glucosinolates are increased in the *serk1-3serk3-2* double mutant, while only CYP79F2 is up-regulated, this is more likely controlled by the increase in expression of the upstream BCAT4 and/or MAM1 enzymes. In line with this, the upstream intermediate 2-oxo-5-methylpentanoate is increased in our analysis. In addition, at least one Trp-derived glucosinolate showed a significantly different level in the double mutant.

It is not clear yet whether this results directly from the SERK-mediated gene regulation or a secondary interaction between the two glucosinolate biosynthetic pathways. Disrupted glucosinolate biosynthesis is known to correlate to severe growth and developmental phenotypes and a disrupted hormone homeostasis (Bak and Feyereisen, 2001; Bak et al., 2001; Smolen and Bender, 2002; Tantikanjana et al., 2004). Via a bioinformatics approach, it was shown that several hormone-related genes, including those of abscisic acid, auxin, BR, cytokinin, ethylene, and jasmonate metabolism, are connected to glucosinolate metabolism (Chen et al., 2011). For example, CYP83B1 is the first committed enzyme of indole glucosinolate biosynthesis. Loss of CYP83B1 function results in an increased flux of indole-3-acetaldoxime into indole-3-acetic acid biosynthesis (Bak and Feyereisen, 2001; Bak et al., 2001), while disrupted jasmonate signaling results in the down-regulation of genes involved in glucosinolate biosynthesis (Chen et al., 2011). It remains to be determined whether, in a wild-type situation, these observations indeed point to physiologically relevant interactions between the different hormone pathways. Proteomics and metabolomics studies of plant lines with reduced CYP79F2 expression resulted in a complex pattern of possible associated processes, including altered levels of other amino acids and sugars, chloroplast dysfunction, oxidative stress, and hormone metabolism (Chen et al., 2012). Altogether, the increased expression of glucosinolate biosynthesis genes in the *serk1-3serk3-2* double mutant may cause a disrupted hormonal homeostasis resulting in a complex pleiotropic phenotype. This would be in line with the phenotypical characterization of the *serk1serk3* double and *serk1serk3serk4* triple mutants (Du et al., 2012). It appears that the root meristem phenotype of the *serk1serk3serk4* triple mutant is more severe when compared with that of the *bri1-701* mutant.

In addition, the expression of cell cycle marker genes (CYCB1;1) and auxin transporters (PINs) is reduced drastically in the *serk1serk3serk4* triple mutant but not in *bri1* mutants (Du et al., 2012). Therefore, Du et al. (2012) postulated that SERKs may affect root development by modulating the expression of root development-related (WOX5 and SHR) and auxin transport-related (PIN) genes, possibly by interacting with another (unknown) receptor-like kinase. The data presented here indicate that a possible mechanism for the observed phenotype in the *serk* mutants, besides the known BR-, abscission-, and cell death-related processes, is the disruption of secondary metabolic processes such as glucosinolate biosynthesis. The BR-deficient mutant *cpd* has an increased glucosinolate content, while plants overexpressing the BR biosynthesis gene DWF4 exhibit an increase in glucosinolate level (Guo et al., 2013). In addition, five of the six MYB transcriptional regulators responsible for activation of the glucosinolate biosynthesis genes, as well as the biosynthesis genes CYP79B2, CYP79B3, CYP79F1, CYP79F2, CYP83A1, and CYP83B1, are significantly down-regulated in the gain-of-BR-function mutants *bes1-D* and *35sBZR1/bzr1-1D* (Guo et al., 2013). For this reason, it has been postulated that BR signaling inhibits glucosinolate biosynthesis. The BR-mediated signaling is impaired in the *serk1-3serk3-2* double mutant; therefore, the up-regulation of the glucosinolate biosynthesis-related genes CYP79F2, MAM1, BCAT4, and CYP83A1 most likely correlates to BRI1-mediated signaling. However, the same set of glucosinolate-related biosynthesis genes also are known to be affected upon defense responses (van de Mortel et al., 2012) and down-regulated upon cytokinin treatment (Brenner et al., 2005). Given the diversity of the glucosinolate biosynthesis pathway and the bidirectional effect of hormone homeostasis/glucosinolate biosynthesis, it is attractive to speculate that the SERK coreceptors affect secondary metabolic processes via multiple signaling pathways.

MATERIALS AND METHODS

Plant Growth Conditions

Arabidopsis (*Arabidopsis thaliana*) ecotype Col-0 was used as the wild-type reference. The *serk1-3* (GABI-KAT line 448E10) and *serk3-2* or *bak1-4* (SALK_116202) single mutants, the *serk1-3serk3-2* double mutants, and the *bri1-301* mutant (Xu et al., 2008), all in the Col-0 background, were used throughout this study. *gpat5-1* and *gpat5-2* mutants have been described (Beisson et al., 2007). Seeds were surface sterilized using ethanol:bleach (4:1, v/v) and germinated on one-half-strength Murashige and Skoog medium (Duchefa) supplemented with 1% Suc (Sigma-Aldrich), 0.1% MES (Sigma-Aldrich), and 0.8% Daishin Agar (Sigma-Aldrich). Seedlings grown for RNA isolation were germinated on growth medium containing 1.2% Daishin Agar. To equalize germination, the plates were kept in the dark at 4°C for 2 d, after which the seedlings were grown vertically under fluorescent light at 22°C with a 16-h-light/8-h-dark photoperiod. For the root growth assays, each measurement consisted of 20 or more roots measured in three independent replicates. To test seed coat permeability, a Tetrazolium Red assay was used according to Beisson et al. (2007).

RNA Isolation and Sample Preparation

Roots of 4-d-old Arabidopsis seedlings were cut just below the hypocotyl and ground in liquid nitrogen. Approximately 100 mg of ground material was dissolved in 1 mL of Trizol reagent (Invitrogen) and incubated for 5 min at room temperature. Next, 200 μL of chloroform was added, and the sample was homogenized, incubated for 2 min, and centrifuged for 15 min at 4°C. After phase separation, isopropanol was added to the aqueous phase, which was incubated subsequently for 10 min at room temperature and further purified using an RNA Easy Mini Kit (Qiagen). Before hybridization on the microarray, the RNA quality was tested using a bioanalyzer. All samples used for microarray analysis were replicated three times in independent biological experiments, and each replication consisted of 3,000 or more seedlings.

qRT-PCR Analysis

RNA was extracted with the RNeasy Kit (Qiagen). Poly(dT) cDNA was prepared from 1 μg of total RNA with an iScript cDNA Synthesis Kit (Bio-Rad) and analyzed on the CFX384 Real-Time PCR detection system (Bio-Rad) with iQ SYBR Green Supermix (Bio-Rad) according to the manufacturer's instructions. Primer pairs were designed with the Beacon Designer 7.0 (Premier Biosoft International). All individual reactions were done in triplicate with two biological replicates. Data were analyzed with qBase (Hellemans et al., 2007). Expression levels were normalized to those of *EEF1α4* and *CDKA1;1*. The primer sequences are listed in Supplemental Table S12.

Metabolite Extraction and Mass Spectrometry

Roots of 4-d-old Arabidopsis seedlings were cut just below the hypocotyl and ground for 30 s at 30 Hz with an MM400 automatic grinder (Retsch) in prefrozen holders. Immediately, 3 μL mg^{-1} ice-cold acidified (0.125% formic acid) aqueous methanol was added to the ground material, and samples were incubated for 2 min on ice. Subsequently, samples were sonicated three times at 40 kHz and 22 μm of amplitude for 15 s using a Soniprep 150 with exponential microprobe (MSE) and centrifuged for 10 min at room temperature. The supernatant was then filtered with a 0.2-μm polytetrafluoroethylene filter and stored at −80°C.

For metabolic analysis, liquid chromatography-mass spectrometry was performed using a 4.6-mm Ø Luna C18 reverse-phase column (Phenomenex) and a microTOF-Q mass spectrometer (Bruker). For the annotation of metabolites, a data-dependent liquid chromatography-tandem mass spectrometry analysis was performed, selecting top 10 peaks in each full mass spectrometry scan, with 12-s dynamic exclusion and a window of 1.5 D, on a Q Exactive hybrid quadrupole orbitrap mass spectrometer (Thermo Fisher Scientific). The following gradient was used in both analyses: 5 min, 5% acetonitrile and 95% water; 40 min, 40% acetonitrile and 60% water; 45 min, 100% acetonitrile and 0% water; and 55 to 65 min, 5% acetonitrile and 95% water. For each data point, three biological replicates were measured three times each to minimize variance.

Genomics and Metabolomics Data Analysis

The scanned Affymetrix GeneChip Arabidopsis Gene 1.0 ST arrays were analyzed using Bioconductor packages (www.bioconductor.org; Gentleman et al., 2004) integrated in the automated online MADMAX pipeline (https://madmax.bioinformatics.nl; Lin et al., 2011). A quantile normalization was used to normalize the array data, and expression estimates were compiled with the RMA method using the empirical Bayes approach (Wu et al., 2004). The arrays were considered as of sufficiently high quality if (1) the fitPLM images have less than 10% of specks and (2) box plots representing the relative long expression and normalized unscaled SE values should not deviate between the arrays. Probe sets that were differentially expressed were identified with linear models, using moderated *t* statistics and empirical Bayes regularization for implementation of the SES (Smyth, 2004). As a control for the variation within the replicates, PCA was performed on normalized intensity values. Given the morphological differences between the *serk1serk3* double mutant and the wild-type seedlings (Du et al., 2012), further analysis was done on genes that were 2-fold differentially regulated compared with the Col-0 lines using an FDR of 1%. For comparison of the differentially regulated genes in the *bri1-301* line with differentially regulated genes in the *bri1-116* line (Sun et al., 2010), the same stringency values as used by Sun et al., 2010 were applied. GeneTrail software (Keller et al., 2008) was employed for ORA and underrepresentation analysis of genes using a minimum of three genes identified per category and default settings for statistics (i.e. an FDR [Benjamini and Hochberg, 1995] for correction of multiple testing and a significance level of 0.05). Differentially regulated genes were binned in different cellular processes using MapMan analysis (Thimm et al., 2004). HCL was done with the TM4 microarray software suite (http://www.tm4.org/mev/) using default settings, which apply a Pearson correlation as a distance measure and an average linkage for clustering. Venn diagrams were made using the R Bioconductor package VennDiagram (Chen and Boutros, 2011).

For differentially regulated genes in the *bri1-116* lines, data were derived from Sun et al. (2010) and downloaded from the GEO2R database using GEO accession numbers GSE25134 using GSM617578 to GSM617580 for the wild-type reference set and GSM617575 to GSM617577 for *bri1-116*. For differentially regulated genes in the *cpr5* mutant, GEO accession number GSE40322 was downloaded, using GSM991297 to GSM991299 for the wild type and GSM991294 to GSM991296 for the *cpr5* mutant. Values for differentially regulated genes were derived from GEO2R using a Benjamin and Hochberg adjustment for multiple testing (FDR) for calculation of the adjusted *P* values (FDR values).

When comparing genes differentially regulated in the *serk1-3serk3-2* double mutant with known processes related to SERK1 and SERK3, the *P* values were calculated using a cumulative hypergeometric distribution:

$$p = \sum_{x=0}^{m-1} \frac{\binom{k}{x}\binom{N-k}{n-x}}{\binom{N}{n}}$$

where N denotes the number of probes on the Affymetrix GeneChip (27827), k is the size of the reference set, n is the number of differentially regulated genes, and m is the number of genes overlapping between groups k and n. The hypergeometric distribution was computed using R version 3.0 (http://www.R-project.org/). The number of genes that can be expected to be identified by chance alone was calculated via:

$$\mathrm{N}_{expected} = \frac{k \times n}{N}$$

Raw data files obtained through mass spectrometry were converted in centroid .mzXML data sets using the ProteoWizard MSConvert tool (Chambers et al., 2012) and visually inspected with Insilicos viewer (www.insilicos.com) to determine the quality of the data sets. Alignment was performed with the xcms online suite (Tautenhahn et al., 2012) using edited HPLC/Bruker Q-TOF negative settings (feature detection of 10 ppm, 10-s minimum peak width, 90-s maximum peak width, noise intensity of 500 units; alignment, bw 15 s; mzwid, 0.03 D). Data analysis was performed on the MetaboAnalyst 3.0 server (Xia et al., 2009, 2012) using the Statistical Analysis tool. Missing data were estimated with KNN, and peak intensities were filtered on relative SD and normalized on total raw signal. Peak intensities were log transformed, to reduce heteroscedasticity, and autoscaled (van den Berg et al., 2006). The SAM and RF methods were applied to identify metabolites that differ significantly between the wild-type and double mutant samples. SAM was performed with a Delta of 1, corresponding to an FDR of 0.03. RF was validated through 10-fold cross-validation. A ranked data table of significantly regulated metabolites was created by pooling the top scoring 50 features from each test, and a new rank was assigned to them based on their average ranks.

Liquid chromatography-tandem mass spectrometry data were annotated using MAGMa (Ridder et al., 2012, 2013) based on candidate molecules retrieved from the KEGG, MetaCyc, and PubChem databases. The best candidates according to the MAGMa penalty score were assigned to each mass peak of interest. Additionally, a query of monoisotopic mass peaks was submitted to the AraCyc database with increasing ppm thresholds (5–50) to identify additional metabolites, assigning the identities with the lowest ppm difference.

Supplemental Data

The following supplemental materials are available.

Supplemental Figure S1. *serk1-3serk3-2* root physiological and molecular phenotypes.

Supplemental Figure S2. PCA of microarray data.

Supplemental Figure S3. Comparison of genes differentially regulated in *serk1-3serk3-2* and BES1/BSR1 target genes.

Supplemental Figure S4. Suberin biosynthesis genes are differentially regulated in the *serk1-3serk3-2* mutant.

Supplemental Table S1. Raw data array 1 for single mutants *serk1-3*, *serk3-2*, and *bri1-301*.

Supplemental Table S2. Raw data array 2 for double mutant *serk1-3/serk3-2* and *bri1-301*.

Supplemental Table S3. Genes differentially regulated in the *serk3-2* single and *serk1-3serk3-2* double mutants.

Supplemental Table S4. Genes differentially regulated in the *serk3-2* mutant analyzed using MapMan.

Supplemental Table S5. Groups defined for genes differentially regulated in *serk1-3serk3-2*.

Supplemental Table S6. Genes differentially regulated in the *bri1-301* mutant with at least $\log_2$ 1.5-fold change and an FDR value of 1%.

Supplemental Table S7. Cutin and suberin biosynthesis genes differentially regulated in the *serk1-3*, *serk3-2*, and *bri-116* mutants.

Supplemental Table S8. Defense-related genes.

Supplemental Table S9. Cell death-related genes.

Supplemental Table S10. Abscission-related genes.

Supplemental Table S11. Core cell cycle genes.

Supplemental Table S12. Primers used for qRT-PCR.

Supplemental File S1. Genes differentially regulated in *serk1-3serk3-2* compared with known BRI1-related genes.

ACKNOWLEDGMENTS

We thank F. Beisson for providing the *gpat5-1* and *gpat5-2* seeds, Jenny Jansen for hybridizing the Affymetrix gene chips and the initial analysis using the MADMAX pipeline, and Dolf Weijers and Bert de Rybel for advice on the data analysis.

Received September 29, 2016; accepted October 28, 2016; published November 1, 2016.

LITERATURE CITED

aan den Toorn M, Albrecht CA, de Vries S (2015) On the origin of SERKs. Mol Plant **8:** 762–782

Albrecht C, Russinova E, Hecht V, Baaijens E, de Vries S (2005) The *Arabidopsis thaliana* SOMATIC EMBRYOGENESIS RECEPTOR-LIKE KINASES1 and 2 control male sporogenesis. Plant Cell **17:** 3337–3349

Albrecht C, Russinova E, Kemmerling B, Kwaaitaal M, de Vries SC (2008) Arabidopsis SOMATIC EMBRYOGENESIS RECEPTOR KINASE proteins serve brassinosteroid-dependent and -independent signaling pathways. Plant Physiol **148:** 611–619

Backes C, Keller A, Kuentzer J, Kneissl B, Comtesse N, Elnakady YA, Müller R, Meese E, Lenhof HP (2007) GeneTrail: advanced gene set enrichment analysis. Nucleic Acids Res **35:** W186–W192

Bak S, Feyereisen R (2001) The involvement of two p450 enzymes, CYP83B1 and CYP83A1, in auxin homeostasis and glucosinolate biosynthesis. Plant Physiol **127:** 108–118

Bak S, Tax FE, Feldmann KA, Galbraith DW, Feyereisen R (2001) CYP83B1, a cytochrome P450 at the metabolic branch point in auxin and indole glucosinolate biosynthesis in *Arabidopsis*. Plant Cell **13:** 101–111

Baxter I, Hosmani PS, Rus A, Lahner B, Borevitz JO, Muthukumar B, Mickelbart MV, Schreiber L, Franke RB, Salt DE (2009) Root suberin forms an extracellular barrier that affects water relations and mineral nutrition in Arabidopsis. PLoS Genet **5:** e1000492

Beisson F, Li Y, Bonaventure G, Pollard M, Ohlrogge JB (2007) The acyltransferase GPAT5 is required for the synthesis of suberin in seed coat and root of *Arabidopsis*. Plant Cell **19:** 351–368

Beisson F, Li-Beisson Y, Pollard M (2012) Solving the puzzles of cutin and suberin polymer biosynthesis. Curr Opin Plant Biol **15:** 329–337

Benjamini Y, Hochberg Y (1995) Controlling the false discovery rate: a practical and powerful approach to multiple testing. J R Stat Soc B **57:** 289–300

Boudsocq M, Willmann MR, McCormack M, Lee H, Shan L, He P, Bush J, Cheng SH, Sheen J (2010) Differential innate immune signalling via Ca^{2+} sensor protein kinases. Nature **464:** 418–422

Bowling SA, Clarke JD, Liu Y, Klessig DF, Dong X (1997) The *cpr5* mutant of *Arabidopsis* expresses both NPR1-dependent and NPR1-independent resistance. Plant Cell **9:** 1573–1584

Brenner WG, Romanov GA, Köllmer I, Bürkle L, Schmülling T (2005) Immediate-early and delayed cytokinin response genes of Arabidopsis thaliana identified by genome-wide expression profiling reveal novel cytokinin-sensitive processes and suggest cytokinin action through transcriptional cascades. Plant J **44:** 314–333

Chambers MC, Maclean B, Burke R, Amodei D, Ruderman DL, Neumann S, Gatto L, Fischer B, Pratt B, Egertson J, et al (2012) A cross-platform toolkit for mass spectrometry and proteomics. Nat Biotechnol **30:** 918–920

Chen H, Boutros PC (2011) VennDiagram: a package for the generation of highly-customizable Venn and Euler diagrams in R. BMC Bioinformatics **12:** 35

Chen S, Glawischnig E, Jørgensen K, Naur P, Jørgensen B, Olsen CE, Hansen CH, Rasmussen H, Pickett JA, Halkier BA (2003) CYP79F1 and CYP79F2 have distinct functions in the biosynthesis of aliphatic glucosinolates in Arabidopsis. Plant J **33:** 923–937

Chen Y, Yan X, Chen S (2011) Bioinformatic analysis of molecular network of glucosinolate biosynthesis. Comput Biol Chem **35:** 10–18

Chen YZ, Pang QY, He Y, Zhu N, Branstrom I, Yan XF, Chen S (2012) Proteomics and metabolomics of Arabidopsis responses to perturbation of glucosinolate biosynthesis. Mol Plant **5:** 1138–1150

Chinchilla D, Shan L, He P, de Vries S, Kemmerling B (2009) One for all: the receptor-associated kinase BAK1. Trends Plant Sci **14:** 535–541

Chinchilla D, Zipfel C, Robatzek S, Kemmerling B, Nürnberger T, Jones JD, Felix G, Boller T (2007) A flagellin-induced complex of the receptor FLS2 and BAK1 initiates plant defence. Nature **448:** 497–500

Cho SK, Larue CT, Chevalier D, Wang H, Jinn TL, Zhang S, Walker JC (2008) Regulation of floral organ abscission in Arabidopsis thaliana. Proc Natl Acad Sci USA **105:** 15629–15634

Chory J, Nagpal P, Peto CA (1991) Phenotypic and genetic analysis of *det2*, a new mutant that affects light-regulated seedling development in *Arabidopsis*. Plant Cell **3:** 445–459

Clouse SD, Langford M, McMorris TC (1996) A brassinosteroid-insensitive mutant in Arabidopsis thaliana exhibits multiple defects in growth and development. Plant Physiol **111:** 671–678

Clouse SD, Sasse JM (1998) Brassinosteroids: essential regulators of plant growth and development. Annu Rev Plant Physiol Plant Mol Biol **49:** 427–451

Deng Z, Zhang X, Tang W, Oses-Prieto JA, Suzuki N, Gendron JM, Chen H, Guan S, Chalkley RJ, Peterman TK, et al (2007) A proteomics study of brassinosteroid response in Arabidopsis. Mol Cell Proteomics **6:** 2058–2071

Denoux C, Galletti R, Mammarella N, Gopalan S, Werck D, De Lorenzo G, Ferrari S, Ausubel FM, Dewdney J (2008) Activation of defense response pathways by OGs and Flg22 elicitors in Arabidopsis seedlings. Mol Plant **1:** 423–445

Domergue F, Vishwanath SJ, Joubès J, Ono J, Lee JA, Bourdon M, Alhattab R, Lowe C, Pascal S, Lessire R, et al (2010) Three Arabidopsis fatty acyl-coenzyme A reductases, FAR1, FAR4, and FAR5, generate primary fatty alcohols associated with suberin deposition. Plant Physiol **153:** 1539–1554

Du J, Yin H, Zhang S, Wei Z, Zhao B, Zhang J, Gou X, Lin H, Li J (2012) Somatic embryogenesis receptor kinases control root development mainly via brassinosteroid-independent actions in Arabidopsis thaliana. J Integr Plant Biol **54:** 388–399

Edgar R, Domrachev M, Lash AE (2002) Gene Expression Omnibus: NCBI gene expression and hybridization array data repository. Nucleic Acids Res **30:** 207–210

Eisen MB, Spellman PT, Brown PO, Botstein D (1998) Cluster analysis and display of genome-wide expression patterns. Proc Natl Acad Sci USA **95:** 14863–14868

Fan M, Wang M, Bai MY (2016) Diverse roles of SERK family genes in plant growth, development and defense response. Sci China Life Sci **59:** 889–896

Fernie AR, Stitt M (2012) On the discordance of metabolomics with proteomics and transcriptomics: coping with increasing complexity in logic,

chemistry, and network interactions scientific correspondence. Plant Physiol **158:** 1139–1145

Gao G, Zhang S, Wang C, Yang X, Wang Y, Su X, Du J, Yang C (2011) Arabidopsis CPR5 independently regulates seed germination and postgermination arrest of development through LOX pathway and ABA signaling. PLoS ONE **6:** e19406

Gentleman RC, Carey VJ, Bates DM, Bolstad B, Dettling M, Dudoit S, Ellis B, Gautier L, Ge Y, Gentry J, et al (2004) Bioconductor: open software development for computational biology and bioinformatics. Genome Biol **5:** R80

González-Carranza ZH, Shahid AA, Zhang L, Liu Y, Ninsuwan U, Roberts JA (2012) A novel approach to dissect the abscission process in Arabidopsis. Plant Physiol **160:** 1342–1356

González-García MP, Vilarrasa-Blasi J, Zhiponova M, Divol F, Mora-García S, Russinova E, Caño-Delgado AI (2011) Brassinosteroids control meristem size by promoting cell cycle progression in Arabidopsis roots. Development **138:** 849–859

Gou X, Yin H, He K, Du J, Yi J, Xu S, Lin H, Clouse SD, Li J (2012) Genetic evidence for an indispensable role of somatic embryogenesis receptor kinases in brassinosteroid signaling. PLoS Genet **8:** e1002452

Guo R, Qian H, Shen W, Liu L, Zhang M, Cai C, Zhao Y, Qiao J, Wang Q (2013) BZR1 and BES1 participate in regulation of glucosinolate biosynthesis by brassinosteroids in Arabidopsis. J Exp Bot **64:** 2401–2412

Hacham Y, Holland N, Butterfield C, Ubeda-Tomas S, Bennett MJ, Chory J, Savaldi-Goldstein S (2011) Brassinosteroid perception in the epidermis controls root meristem size. Development **138:** 839–848

Halkier BA, Gershenzon J (2006) Biology and biochemistry of glucosinolates. Annu Rev Plant Biol **57:** 303–333

Hanssen IM, van Esse HP, Ballester AR, Hogewoning SW, Parra NO, Paeleman A, Lievens B, Bovy AG, Thomma BP (2011) Differential tomato transcriptomic responses induced by pepino mosaic virus isolates with differential aggressiveness. Plant Physiol **156:** 301–318

He K, Gou X, Yuan T, Lin H, Asami T, Yoshida S, Russell SD, Li J (2007) BAK1 and BKK1 regulate brassinosteroid-dependent growth and brassinosteroid-independent cell-death pathways. Curr Biol **17:** 1109–1115

Hecht V, Vielle-Calzada JP, Hartog MV, Schmidt ED, Boutilier K, Grossniklaus U, de Vries SC (2001) The Arabidopsis SOMATIC EMBRYOGENESIS RECEPTOR KINASE 1 gene is expressed in developing ovules and embryos and enhances embryogenic competence in culture. Plant Physiol **127:** 803–816

Heese A, Hann DR, Gimenez-Ibanez S, Jones AME, He K, Li J, Schroeder JI, Peck SC, Rathjen JP (2007) The receptor-like kinase SERK3/BAK1 is a central regulator of innate immunity in plants. Proc Natl Acad Sci USA **104:** 12217–12222

Hellemans J, Mortier G, De Paepe A, Speleman F, Vandesompele J (2007) qBase relative quantification framework and software for management and automated analysis of real-time quantitative PCR data. Genome Biol **8:** R19

Hennig L, Menges M, Murray JA, Gruissem W (2003) Arabidopsis transcript profiling on Affymetrix GeneChip arrays. Plant Mol Biol **53:** 457–465

Höfer R, Briesen I, Beck M, Pinot F, Schreiber L, Franke R (2008) The Arabidopsis cytochrome P450 CYP86A1 encodes a fatty acid omega-hydroxylase involved in suberin monomer biosynthesis. J Exp Bot **59:** 2347–2360

Jeong YJ, Shang Y, Kim BH, Kim SY, Song JH, Lee JS, Lee MM, Li J, Nam KH (2010) BAK7 displays unequal genetic redundancy with BAK1 in brassinosteroid signaling and early senescence in Arabidopsis. Mol Cells **29:** 259–266

Jinn TL, Stone JM, Walker JC (2000) HAESA, an Arabidopsis leucine-rich repeat receptor kinase, controls floral organ abscission. Genes Dev **14:** 108–117

Karlova R, Boeren S, Russinova E, Aker J, Vervoort J, de Vries S (2006) The *Arabidopsis* SOMATIC EMBRYOGENESIS RECEPTOR-LIKE KINASE1 protein complex includes BRASSINOSTEROID-INSENSITIVE1. Plant Cell **18:** 626–638

Keller A, Backes C, Al-Awadhi M, Gerasch A, Küntzer J, Kohlbacher O, Kaufmann M, Lenhof HP (2008) GeneTrailExpress: a web-based pipeline for the statistical evaluation of microarray experiments. BMC Bioinformatics **9:** 552

Kirik V, Bouyer D, Schöbinger U, Bechtold N, Herzog M, Bonneville JM, Hülskamp M (2001) CPR5 is involved in cell proliferation and cell death control and encodes a novel transmembrane protein. Curr Biol **11:** 1891–1895

Knoke B, Textor S, Gershenzon J, Schuster S (2009) Mathematical modelling of aliphatic glucosinolates chain length distribution in *Arabidopsis thaliana* leaves. Phytochem Rev **8:** 39–51

Kobayashi K, Baba S, Obayashi T, Sato M, Toyooka K, Keränen M, Aro EM, Fukaki H, Ohta H, Sugimoto K, et al (2012) Regulation of root greening by light and auxin/cytokinin signaling in *Arabidopsis*. Plant Cell **24:** 1081–1095

Kumpf RP, Shi CL, Larrieu A, Stø IM, Butenko MA, Péret B, Riiser ES, Bennett MJ, Aalen RB (2013) Floral organ abscission peptide IDA and its HAE/HSL2 receptors control cell separation during lateral root emergence. Proc Natl Acad Sci USA **110:** 5235–5240

Lamesch P, Berardini TZ, Li D, Swarbreck D, Wilks C, Sasidharan R, Muller R, Dreher K, Alexander DL, Garcia-Hernandez M, et al (2012) The Arabidopsis Information Resource (TAIR): improved gene annotation and new tools. Nucleic Acids Res **40:** D1202–D1210

Lewis MW, Leslie ME, Fulcher EH, Darnielle L, Healy PN, Youn JY, Liljegren SJ (2010) The SERK1 receptor-like kinase regulates organ separation in Arabidopsis flowers. Plant J **62:** 817–828

Li J, Wen J, Lease KA, Doke JT, Tax FE, Walker JC (2002) BAK1, an Arabidopsis LRR receptor-like protein kinase, interacts with BRI1 and modulates brassinosteroid signaling. Cell **110:** 213–222

Li Y, Beisson F, Koo AJ, Molina I, Pollard M, Ohlrogge J (2007) Identification of acyltransferases required for cutin biosynthesis and production of cutin with suberin-like monomers. Proc Natl Acad Sci USA **104:** 18339–18344

Lin K, Kools H, de Groot PJ, Gavai AK, Basnet RK, Cheng F, Wu J, Wang X, Lommen A, Hooiveld GJ, et al (2011) MADMAX: management and analysis database for multiple ~omics experiments. J Integr Bioinform **8:** 160

Luo XM, Lin WH, Zhu S, Zhu JY, Sun Y, Fan XY, Cheng M, Hao Y, Oh E, Tian M, et al (2010) Integration of light- and brassinosteroid-signaling pathways by a GATA transcription factor in Arabidopsis. Dev Cell **19:** 872–883

Masubelele NH, Dewitte W, Menges M, Maughan S, Collins C, Huntley R, Nieuwland J, Scofield S, Murray JA (2005) D-type cyclins activate division in the root apex to promote seed germination in Arabidopsis. Proc Natl Acad Sci USA **102:** 15694–15699

Meng X, Chen X, Mang H, Liu C, Yu X, Gao X, Torii KU, He P, Shan L (2015) Differential function of Arabidopsis SERK family receptor-like kinases in stomatal patterning. Curr Biol **25:** 2361–2372

Meng X, Zhou J, Tang J, Li B, de Oliveira MVV, Chai J, He P, Shan L (2016) Ligand-induced receptor-like kinase complex regulates floral organ abscission in Arabidopsis. Cell Rep **14:** 1330–1338

Nam KH, Li J (2002) BRI1/BAK1, a receptor kinase pair mediating brassinosteroid signaling. Cell **110:** 203–212

Niederhuth CE, Patharkar OR, Walker JC (2013) Transcriptional profiling of the Arabidopsis abscission mutant hae hsl2 by RNA-Seq. BMC Genomics **14:** 37

Olson-Manning CF, Lee CR, Rausher MD, Mitchell-Olds T (2013) Evolution of flux control in the glucosinolate pathway in *Arabidopsis thaliana*. Mol Biol Evol **30:** 14–23

Patterson SE (2001) Cutting loose: abscission and dehiscence in Arabidopsis. Plant Physiol **126:** 494–500

Ridder L, van der Hooft JJJ, Verhoeven S, de Vos RCH, Bino RJ, Vervoort J (2013) Automatic chemical structure annotation of an LC-MS(^{n}) based metabolic profile from green tea. Anal Chem **85:** 6033–6040

Ridder L, van der Hooft JJJ, Verhoeven S, de Vos RCH, van Schaik R, Vervoort J (2012) Substructure-based annotation of high-resolution multistage MS(n) spectral trees. Rapid Commun Mass Spectrom **26:** 2461–2471

Roberts JA, Whitelaw CA, Gonzalez-Carranza ZH, McManus MT (2000) Cell separation processes in plants: models, mechanisms and manipulation. Ann Bot (Lond) **86:** 223–235

Roux M, Schwessinger B, Albrecht C, Chinchilla D, Jones A, Holton N, Malinovsky FG, Tör M, de Vries S, Zipfel C (2011) The *Arabidopsis* leucine-rich repeat receptor-like kinases BAK1/SERK3 and BKK1/SERK4 are required for innate immunity to hemibiotrophic and biotrophic pathogens. Plant Cell **23:** 2440–2455

Santiago J, Henzler C, Hothorn M (2013) Molecular mechanism for plant steroid receptor activation by somatic embryogenesis co-receptor kinases. Science **341:** 889–892

Smolen G, Bender J (2002) Arabidopsis cytochrome P450 cyp83B1 mutations activate the tryptophan biosynthetic pathway. Genetics **160:** 323–332

Smyth GK (2004) Linear models and empirical Bayes methods for assessing differential expression in microarray experiments. Stat Appl Genet Mol Biol **3:** Article3

Sønderby IE, Geu-Flores F, Halkier BA (2010) Biosynthesis of glucosinolates: gene discovery and beyond. Trends Plant Sci **15:** 283–290

Song L, Zhou XY, Li L, Xue LJ, Yang X, Xue HW (2009) Genome-wide analysis revealed the complex regulatory network of brassinosteroid effects in photomorphogenesis. Mol Plant **2:** 755–772

Stenvik GE, Tandstad NM, Guo Y, Shi CL, Kristiansen W, Holmgren A, Clark SE, Aalen RB, Butenko MA (2008) The EPIP peptide of INFLORESCENCE DEFICIENT IN ABSCISSION is sufficient to induce abscission in *Arabidopsis* through the receptor-like kinases HAESA and HAESA-LIKE2. Plant Cell **20:** 1805–1817

Sun L, van Nocker S (2010) Analysis of promoter activity of members of the PECTATE LYASE-LIKE (PLL) gene family in cell separation in Arabidopsis. BMC Plant Biol **10:** 152

Sun Y, Fan XY, Cao DM, Tang W, He K, Zhu JY, He JX, Bai MY, Zhu S, Oh E, et al (2010) Integration of brassinosteroid signal transduction with the transcription network for plant growth regulation in Arabidopsis. Dev Cell **19:** 765–777

Sun Y, Han Z, Tang J, Hu Z, Chai C, Zhou B, Chai J (2013) Structure reveals that BAK1 as a co-receptor recognizes the BRI1-bound brassinolide. Cell Res **23:** 1326–1329

Tantikanjana T, Mikkelsen MD, Hussain M, Halkier BA, Sundaresan V (2004) Functional analysis of the tandem-duplicated P450 genes SPS/BUS/CYP79F1 and CYP79F2 in glucosinolate biosynthesis and plant development by Ds transposition-generated double mutants. Plant Physiol **135:** 840–848

Tautenhahn R, Patti GJ, Rinehart D, Siuzdak G (2012) XCMS Online: a web-based platform to process untargeted metabolomic data. Anal Chem **84:** 5035–5039

Thimm O, Bläsing O, Gibon Y, Nagel A, Meyer S, Krüger P, Selbig J, Müller LA, Rhee SY, Stitt M (2004) MAPMAN: a user-driven tool to display genomics data sets onto diagrams of metabolic pathways and other biological processes. Plant J **37:** 914–939

van de Mortel JE, de Vos RC, Dekkers E, Pineda A, Guillod L, Bouwmeester K, van Loon JJ, Dicke M, Raaijmakers JM (2012) Metabolic and transcriptomic changes induced in Arabidopsis by the rhizobacterium Pseudomonas fluorescens SS101. Plant Physiol **160:** 2173–2188

van den Berg RA, Hoefsloot HCJ, Westerhuis JA, Smilde AK, van der Werf MJ (2006) Centering, scaling, and transformations: improving the biological information content of metabolomics data. BMC Genomics **7:** 142–156

Vandepoele K, Raesa J, De Veyldera L, Rouzé P, Rombautsa S, Inzé D (2002) Genome-wide analysis of core cell cycle genes in Arabidopsis. Plant Cell **14:** 903–916

van Esse GW, van Mourik S, Albrecht C, van Leeuwen J, de Vries SC (2013) A mathematical model for the coreceptors SOMATIC EMBRYOGENESIS RECEPTOR-LIKE KINASE1 and SOMATIC EMBRYOGENESIS RECEPTOR-LIKE KINASE3 in BRASSINOSTEROID INSENSITIVE1-mediated signaling. Plant Physiol **163:** 1472–1481

van Esse GW, van Mourik S, Stigter H, ten Hove CA, Molenaar J, de Vries SC (2012) A mathematical model for BRASSINOSTEROID INSENSITIVE1-mediated signaling in root growth and hypocotyl elongation. Plant Physiol **160:** 523–532

van Esse HP, Fradin EF, de Groot PJ, de Wit PJGM, Thomma BPHJ (2009) Tomato transcriptional responses to a foliar and a vascular fungal pathogen are distinct. Mol Plant Microbe Interact **22:** 245–258

Vishwanath SJ, Delude C, Domergue F, Rowland O (2015) Suberin: biosynthesis, regulation, and polymer assembly of a protective extracellular barrier. Plant Cell Rep **34:** 573–586

Wang J, Li H, Han Z, Zhang H, Wang T, Lin G, Chang J, Yang W, Chai J (2015) Allosteric receptor activation by the plant peptide hormone phytosulfokine. Nature **525:** 265–268

Wang ZY, Bai MY, Oh E, Zhu JY (2012) Brassinosteroid signaling network and regulation of photomorphogenesis. Annu Rev Genet **46:** 701–724

Wang ZY, Seto H, Fujioka S, Yoshida S, Chory J (2001) BRI1 is a critical component of a plasma-membrane receptor for plant steroids. Nature **410:** 380–383

Wolf S, Mravec J, Greiner S, Mouille G, Höfte H (2012) Plant cell wall homeostasis is mediated by brassinosteroid feedback signaling. Curr Biol **22:** 1732–1737

Wu Z, Irizarry RA, Gentleman R, Martinez-Murillo F, Spencer F (2004) A model-based background adjustment for oligonucleotide expression arrays. J Am Stat Assoc **99:** 909–917

Xia J, Mandal R, Sinelnikov IV, Broadhurst D, Wishart DS (2012) MetaboAnalyst 2.0: a comprehensive server for metabolomic data analysis. Nucleic Acids Res **40:** W127–W133

Xia J, Psychogios N, Young N, Wishart DS (2009) MetaboAnalyst: a web server for metabolomic data analysis and interpretation. Nucleic Acids Res **37:** W652–W660

Xu W, Huang J, Li B, Li J, Wang Y (2008) Is kinase activity essential for biological functions of BRI1? Cell Res **18:** 472–478

Yu X, Li L, Zola J, Aluru M, Ye H, Foudree A, Guo H, Anderson S, Aluru S, Liu P, et al (2011) A brassinosteroid transcriptional network revealed by genome-wide identification of BESI target genes in Arabidopsis thaliana. Plant J **65:** 634–646

Zipfel C, Robatzek S, Navarro L, Oakeley EJ, Jones JD, Felix G, Boller T (2004) Bacterial disease resistance in Arabidopsis through flagellin perception. Nature **428:** 764–767